CORROSION RESISTANCE OF 2205 DUPLEX STAINLESS STEEL IN NORMAL SALINE SOLUTION UNDER SIMULATED INFLAMMATORY CONDITIONS

Asma Sharfeddin, Hesham Mraied, Esra Trok

Department of Materials and Metallurgical Engineering, University of Tripoli
E-mail: a.sharfeddin@uot.edu.ly

Received 10 June 2023; revised 17 July 2023; accepted 7 August 2023

الملخص

تدخل أنواع مختلفة من الفولاذ الأوستنيتي المقاوم للصدأ مثل 316L, 316LMV والفولاذ الأوستنيتي المقاوم للصدأ الخالي من النيكل والغني بالنيتروجين في التطبيقات الطبية الحيوية، نظراً لتوافقها الحيوي، وخصائصها الميكانيكية المناسبة، ومقاومتها العالية للتآكل. لكن اظهر الفولاذ الأوستنيتي المقاوم للصدأ انخفاضاً في مقاومة التآكل عند اختباره في محاليل بيولوجية تحتوي على بيروكسيد الهيدروجين لمحاكاة ظروف الالتهاب داخل الجسم.

في هذه الدراسة، تم تقديم الفولاذ المزدوج المقاوم للصدأ (DSS 2205) كمرشح بديل للفولاذ الأوستنيتي المقاوم للصدأ للتطبيقات الطبية الحيوية. تم فحص سلوك تآكل الفولاذ المزدوج المقاوم للصدأ في محلول ملحي عادي. بمحاكاة تأثير إضافة كل من بيروكسيد الهيدروجين، وهو نوع من الأكسجين التفاعلي وجوده يحاكي حالة التهاب، وكذلك وجود الزلال (الألبومين)، وهو بروتين موجود بوفرة في البيئة البيولوجية .تمت دراسة سلوك التآكل عن طريق الاستقطاب الديناميكي الفعال والتحليل الطيفي للمقاومة الكهروكيميائية. وجد أن معدل تآكل الفولاذ المزدوج المقاوم للصدأ انخفض بشكل ملحوظ في وجود بيروكسيد الهيدروجين، في حين أن إضافة الألبومين لم يغير بشكل كبير من مقاومة التآكل للسبيكة.

أظهرت اختبارات التحليل الطيفي للمقاومة الكهروكيميائية زيادة في سمك طبقة الاكسيد للفولاذ نتيجة إضافة بيروكسيد الهيدروجين. كما أظهرت تجارب الاستقطاب الديناميكي الفعال أن بيروكسيد الهيدروجين، وإلى حد ما الألبومين يعملان كمثبط انودي كما يتضح من تحول قيم جهد التآكل نحو قيم موجبة وكثافة تيار التآكل نحو قيم أصغر.

ABSTRACT

Different grades of austenitic stainless steels such as 316L, 316LMV, and nickel free-high nitrogen austenitic stainless steels have been introduced for biomedical applications, owing to their biocompatibility, suitable mechanical properties and corrosion resistance. When tested in solutions containing hydrogen peroxide to simulate inflammatory conditions, austenitic stainless steels showed decrease in corrosion resistance.

In this study, 2205 duplex stainless steel was introduced as an alternative candidate for austenitic stainless steel for biomedical applications. The corrosion behavior of 2205 duplex stainless steel was investigated in normal saline solution. The effects of addition of hydrogen peroxide, a reactive oxygen species, simulating an inflammatory condition, and addition of human albumin, a protein found in the biological environment, were simulated.

The corrosion behavior was studied by potentiodynamic polarization and electrochemical impedance spectroscopy. It was found that the corrosion rate of the 2205 duplex stainless steel significantly decreased in the presence of hydrogen peroxide, while the addition of human albumin did not significantly alter the corrosion resistance of the alloy.

Electrochemical impedance spectroscopy tests showed the increase in the thickness of the passive film of the steel as a result of addition of hydrogen peroxide. Potentiodynamic polarization experiments showed that hydrogen peroxide, and to a lower extent, human albumin served as an anodic inhibitor as indicated by the shift of corrosion potential towards more positive values and the corrosion current density towards lower values.

KEYWORDS: Duplex Stainless Steel; Corrosion; EIS; Polarization; Constant Phase Element.

INTRODUCTION

It is mandatory for any material to be implanted in a human body to be biocompatible. If not, the presence of this material may cause adverse effects like inflammation, allergy and toxicity either. Once implanted, biomaterials should withstand the mechanical forces that may cause fracture. Furthermore, biomaterials should possess very high corrosion and wear resistance in a physiological environment [1].

Austenitic stainless steels (ASS), such as grades 316L and 316LMV, have been widely used as biomaterials for the manufacturing of orthopedic implants in fracture fixations and joint replacements [2]. It has been found that implants made of ASS when subjected to chloride containing media are prone to different localized corrosion attacks such as pitting, crevice corrosion, and stress corrosion cracking [2,3]. The presence of microorganisms on the surface of the metal will alter the concentration of the different species in the electrolyte, pH and oxygen level, which may result in severe localized corrosion [4]. The release of metallic ions such as Ni (in concentrations higher than those admissible) to human tissue as a result of degradation of the implant can cause metal allergy, carcinogenicity, cytotoxicity and genotoxicity [5-7].

Different approaches were made to enhance the corrosion resistance of stainless steel by minimizing the content of nonmetallic inclusions (chromium carbide). For example vacuum arc re-melting and increase the content of chromium, molybdenum, and nitrogen were found to enhance passivity and resistance to localized corrosion [8-11]. Other materials including Ti and CO-Cr-Mo were found to have better corrosion resistance in biological environments when compared to ASS [1, 12].

Duplex stainless steel (DSS) is gaining more attention to be considered as an alternative to ASS owing to its high resistance to stress corrosion cracking, corrosion fatigue, and pitting corrosion due to the high Cr content in combination with Mo and Ni. DSS also has adequate mechanical properties necessary for implant elaboration due to the coexistence of both delta-ferrite and austenite phases [3,13,14]. The corrosion behaviors of ASS and DSS in physiological environments have been studied elsewhere. Kocijan et al. [15] found that the DSS 2205 had a wider passivation range than the AISI 316L when tested in artificial saliva and a simulated physiological solution using cyclic voltammetry and potentiodynamic measurements. Conradi et al. [14] studied the localized corrosion of AISI 316L and DSS 2205 stainless steel using atomic force microscopy in different physiological environments. The results indicated higher corrosion resistance of DSS 2205 steel as illustrated by the AFM topography analysis.

The composition of the physiological environment into which biomaterials are implanted varies from one site to another in the human body. In general, the environment contains different types of organic and inorganic species such as ions, amino acids, proteins and living cells. The deterioration of the biomaterial as well as inflammation conditions can alter the composition of the environment [16].

Different biocompatible materials like Ti, CoCr, and high nitrogen steel have been found to exhibit different corrosion behaviors depending on the presence or absence of various physiological species in simulated physiological environments. The effects of pH, the presence of certain inorganic species such as hydrogen peroxide (H_2O_2), which will be termed as HP hereafter, or fluoride ions, the presence of organic species such as lipopolysaccharide (LPS), and proteins like albumin on corrosion behavior of metallic biomaterials has been documented in literature [16,17]. The activities of Reactive Oxygen Species (ROS) are associated with some medical conditions such as oxidative stress which can lead to different diseases and disorders including cardiovascular disease, cancer, aging, and various neurodegenerative diseases

HP is one of the ROS species present in vivo and has been used to simulate inflammatory conditions. HP is produced by activated phagocytes and leukocytes and the subsequent formation of hydroxyl radicals, singlet oxygen, and additional HP. Albumin is the most abundant protein in the human body, accounting for about 4% of total protein content. The concentration of albumin in the blood has been used as a major index in health and disease over the years. Structural and functional impairments in albumin are attributed to various pathophysiological conditions like diabetes, osteoarthritis and advanced liver diseases[16].

The objective of this work is to investigate the corrosion behavior of 2205 duplex stainless steel as a candidate material to replace ASS in biological application. Corrosion resistance was examined using Electrochemical Impedance Spectroscopy (EIS) and Potentiodynamic polarization (PD) in a simulated biological environment with and without the addition of hydrogen peroxide and human albumin to simulate conditions of inflammation.

EXPERIMENTAL PROCEDURE

Materials Synthesis and Characterization

The material used in this work was cut from a sheet (0.2 cm thickness) of 2205 duplex stainless steel. The chemical composition (in mass fractions, wt.%) was 22 Cr, 5.5 Ni, 3.2 Mo, 0.18 N, 0.03 C, 0.03 P, 0.02 S, and Fe (balance). For microstructural analysis, samples with an area of 1 cm^2 were cut then mounted in epoxy resin. For electrochemical testing, the sheet was cut into 3x3cm^2 squares using a shear cutting machine. Prior to microstructural analysis and electrochemical testing, samples were mechanically ground with a set of SiC papers down to 1200 grit, polished, degreased with acetone and alcohol, cleaned with di-water, and finally air dried. The microstructure was studied by etching a polished sample with carpenter solution (15 mL HCl and 85 mL ethanol) using Leica optical microscope.

Electrochemical Tests

All electrochemical measurements were performed using a Gamry Reference 600® potentiostat with the conventional three electrode configuration in naturally aerated and stagnant normal saline solution (0.9 % NaCl) having a pH of 5.6. In order to simulate inflammatory conditions, the normal saline solution was doped with either 8 mL/L HP (30% concentration), 8 mL/L human albumin (2% concentration), and (HP + human albumin). Electrochemical tests were carried out in the three electrode electrochemical cell configuration using Gamry paint cell unit used for flat plate samples as shown in Figure (1). The sample, graphite rod, and a commercial saturated calomel electrode (saturated KCl internal solution) were used as the working, counter, and reference electrode, respectively. EIS tests were conducted after 60 min of immersion in the

electrolyte at open circuit potential (E_{OC}) in the frequency range of 10 kHz to 10 MHz, 5 points per decade, and 10 mV_{rms} sinusoidal potential excitation. PD measurements were conducted at a constant scan rate of 0.167 mV/s, starting from E_{OC} to a cathodic potential (-300 mV) up to anodic potential (+300 mV). The obtained data was then fitted using Gamry E-chem software. All electrochemical tests were conducted at room temperature and to ensure data reproducibility and accuracy, the results of minimum three samples are reported for each electrochemical test.

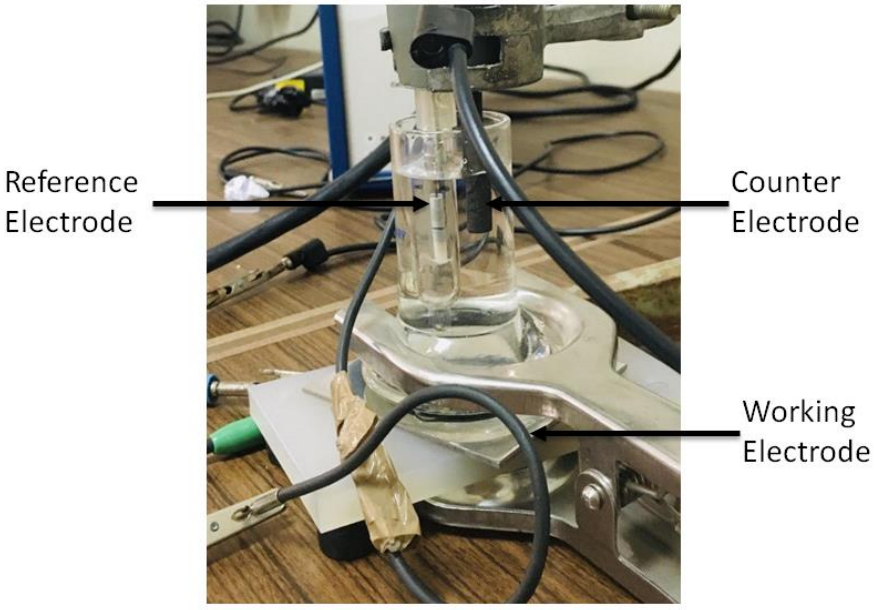

Figure 1: Three electrode electrochemical cell configuration using Gamry paint cell unit used for flat plate samples

RESULTS AND DISCUSSION

Microstructural Characterization:

The microstructure of the studied material is shown in Figure (2). The microstructure consists of about 50% ferrite (α) and 50% austenite (γ). The figure indicates that the austenitic phase is embedded in the ferritic matrix.

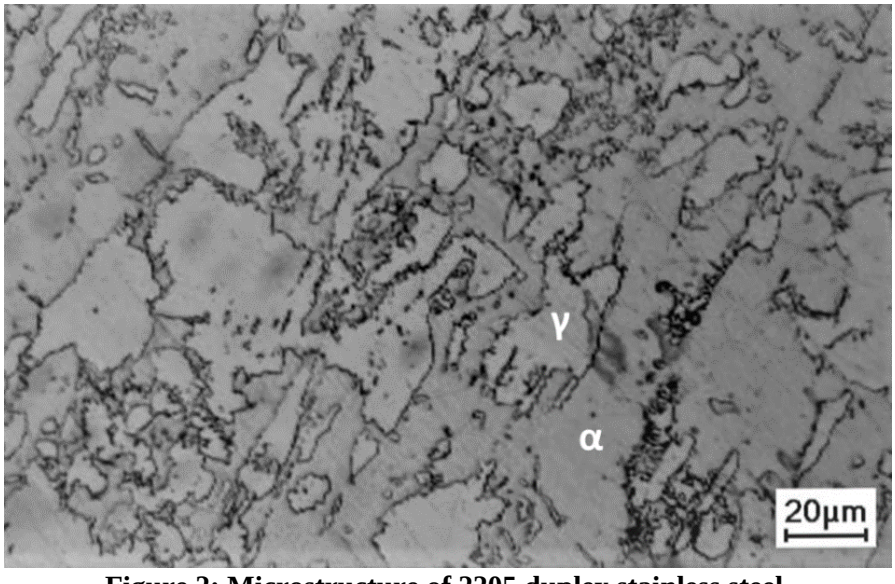

Figure 2: Microstructure of 2205 duplex stainless steel.

Electrochemical Impedance Spectroscopy (EIS) Study

To evaluate the electrochemical kinetics at the sample-electrolyte interface, EIS measurements were conducted after E_{OC} stabilization for 1 hour in normal saline solution and normal saline solution doped with either HP, human, and (HP + human albumin).

The Nyquist diagram for representative results is shown in Figure (3). The plots in the diagram were generally similar in having a single capacitive loop shape, indicating the formation of a protective passive film on the metal surface. This shape can also be expected from a polarization resistance due to Faradaic processes coupled with an interfacial charge storage process. When compared with that of the bare saline solution, the capacitive semicircle of the Nyquist plot becomes larger with the presence of HP, indicating the enhancement of the corrosion resistance. The addition of human albumin did not change the diameter of the semicircles hence did not alter the corrosion resistance of the stainless steel. The capacitive semicircles in the presence of HP and (H_2O_2 + human albumin) are similar in size, indicating that the enhanced corrosion resistance is mainly the result of the addition of HP not the human albumin.

The experimental data were interpreted using the analog equivalent circuit model shown as an inset in Figure (3). This simplified Randles cell includes a solution resistance (Rs), a double layer capacitor in the form of constant phase element (CPE) in parallel with the charge transfer resistance (R_{CT}). The (CPE) was used taking in consideration the non-ideal capacitance behavior resulting from either surface heterogeneity or disturbed time constant of charge transfer reactions [18].

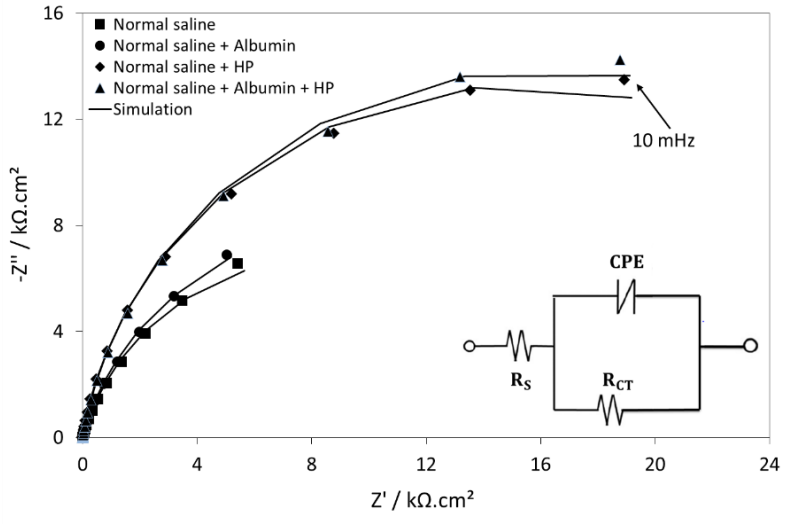

Figure 3: Representative Nyquist plots (scattered data) of 2205 DSS conducted after EOC stabilization for 1 hour in normal saline solution with and without the addition of HP and albumin. The bottom right inset shows the equivalent circuit model used to fit the experimental data, as represented by the solid lines in the Nyquist plots.

The impedance of the non-ideal capacitance CPE is represented as:

$$Z_{CPE} = Y_o^{-1}(j\omega)^{-n} \quad (1)$$

where Y_o is a constant representing a base admittance, $j = (-1)^{1/2}$, ω is the angular frequency, and n is a frequency dependence exponent which measures the deviation from ideal capacitor behavior. The values of n are between 0 and 1. The CPE reduces to a simple capacitor with $C = Y_o$ when n=1. The numeric value of Y_o is roughly indicative of

an effective interfacial capacitance, disregarding dimensional issues. As shown in Figure (3), the fitted results closely matched the experimental behavior for almost all of the frequency range for all results.

The Rs of all electrolytes was in the range of 60 ± 4 Ω.cm2. As expected, the values are consistent with the cell dimensions and electrolyte resistivity and independent of the material tested and electrolyte type. It should be noted here that when the R_{CT} is much larger than the Rs, the later will not appear in Nyquist plots.

Figure (4) shows the values of the parameters of the CPE elements (n and Y_o) obtained from fitting EIS data with the equivalent circuit shown in Figure (3). As shown in Figure (4a), the values of (n) increased due to the addition of human albumin and HP to the normal saline. The value of (n) provides an indication of the capacitive behavior (surface inhomogeneity) of the steel at the interface with the electrolyte. Therefore, this increase in (n) could be related to the strengthening of the capacitive interface as the passive film of the steel becomes smoother and less conductive with the decrease in number of pits [19]. As shown in Figure (4b). The values of Y_o did not change when human albumin was added to the normal saline solution. The decrease was found to occur due to the addition of HP. A decrease in the Y_o (effective interfacial capacitance) can be related to the increase in the thickness of the passive film formed on the surface of the sample [20].

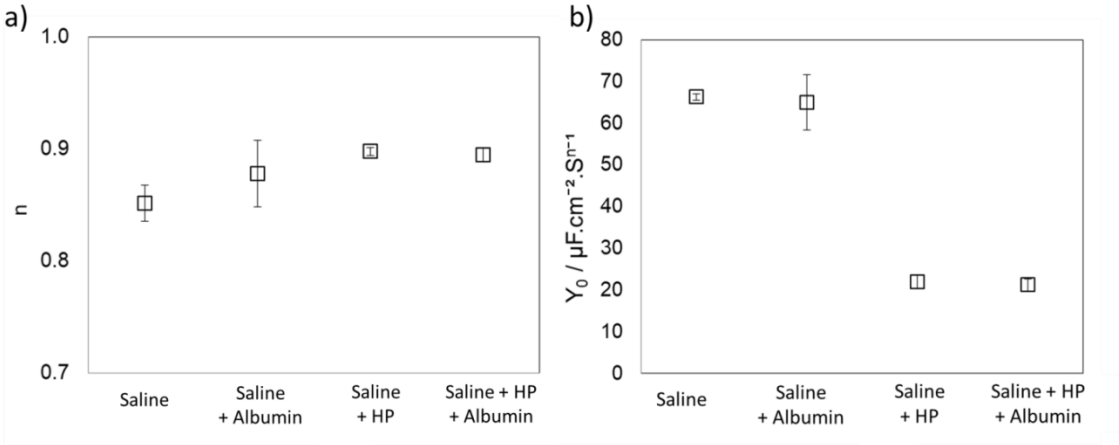

Figure 4: Magnitudes derived fromEIS tests (a) n, (b) Y_O of 2205 DSS after immersion in the different electrolytes. The error bars represent the standard deviation of data.

As (n) approaches the value of 1, the CPE parameter Y_o may be viewed as a rough estimate of the film capacitance C via

$$C = Y_o . sec^{n-1} \quad (2)$$

recognizing that the expression becomes increasingly inaccurate as (n) decreases from unity [21]. A nominal thickness of the passive film (d) may be obtained from the following equation [21]

$$d = \varepsilon \varepsilon_o A/C \quad (3)$$

where ε is the dielectric constant of the passive film (taking it to be ~15.6 for stainless steel, ε_o is the permittivity of vacuum (8.85 x 10^{-14} F.cm^{-1}) and A is the exposed surface area (~15 cm^2, calculated from the diameter of the O-Ring of the Gamry paint cell unit). Equation 3 supports the finding shown in Figure (4). Since C (or Y_o) is inversely

proportional to the thickness of the protective layer (d), the decrease in the capacitance by addition of HP resulted in an increase in the thickness of the protective layer.

The passive film thickness (d) of 2205 duplex stainless steel when exposed to normal saline and normal saline doped with human albumin was (2.7 ± 0.15 nm). These values are comparable to those reported in other investigations for oxide films formed on steel surfaces in different media [19,22], thus supportive of the interpretation of the constant phase element parameters represented in equations 1 through 3.

The thickness of the passive film increased to (8.4 ± 0.6 nm) when normal saline was doped with HP. The same thickness increase resulted from the addition of both human albumin and HP, indicating that this increase is solely associated with the addition of HP.

The decomposition of HP to water in aerated media (equation 4 and 5) catalyzes the formation of metal oxide by providing additional species for the oxygen reduction reaction (equation 6). This would result in the growth of the oxide film [17].

$$2H_2O_2 \rightarrow O_2 + 2H_2O \quad (4)$$

$$H_2O_2 + 2H^+ + 2e^- \rightarrow 2H_2O \quad (5)$$

$$O_2 + 4H^+ + 4e^- \rightarrow 2H_2O \quad (6)$$

The R_{CT} of 2205 DSS was 220 ± 28kΩ.cm^2, when exposed to normal saline. When normal saline was doped with albumin, R_{CT} did not show any significant change with a value of 230 ± 27kΩ.cm^2. When Normal saline was doped with HP, R_{CT} was found to significantly increase to 406 ± 67 kΩ.cm^2. R_{CT} was found to be 470 ± 46kΩ.cm^2 when normal saline was doped with (HP + human albumin). This again confirms that the enhancement in charge transfer resistance is mainly the result of the addition of HP. Indicating that the addition of HP reduced the electrochemical reactions occurring at the metal surface.

The corrosion current density (i_{corr}) from EIS tests was estimated from the R_{CT} using Stern-Geary equation: [23, 24]:-

$$i_{corr} = B/R_{CT} \quad (7)$$

where B is the apparent Stern-Geary coefficient which can be estimated from [23,24]:

$$B = \frac{\beta_a.\beta_c}{2.3(\beta_a+\beta_c)} \quad (8)$$

where β_a and β_c are the anodic and cathodic Tafel slopes, respectively measured from cyclic potentiodynamic polarization experiments. The validity of corrosion current densities estimated from Stern-Geary equation depends on the correct determination of the coefficient B and whether a metal (M) dissolves directly to M^{2+} or through an M^+ intermediate [24-26]. In this work, the value of B was chosen to be equal to 0.026 V, representing the condition of an active metal dissolution. i_{corr} was converted to corrosion rate (C.R) in micrometer per year as shown in Figure (4) using Faraday's conversion (1 μA.cm^{-2} ≈ 10 μm/y), a typical value measured for many engineering materials assuming uniform corrosion for the different components of the alloy [27].

As shown in Figure (5), the values of nominal corrosion rate estimated from EIS did not significantly change by the addition of human albumin. The addition of HP to normal saline solution decreased the corrosion rate by about 45%. The additional slight reduction of corrosion rate when normal saline solution was doped with (HP + human albumin) should be considered as well.

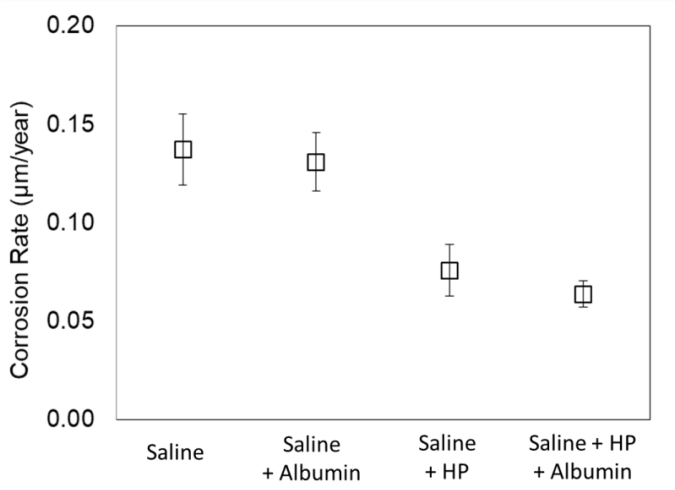

Figure 5: Corrosion rate of 2205 DSS in different electrolytes derived from EIS results. The error bars represent the standard deviation of data.

Potentiodynamic Polarization Experiments:

Figure (6) shows the representative potentiodynamic polarization curves of 2205 DSS after 1-hour immersion in normal saline solution, normal saline solution doped with 8 ml/L albumin, and normal saline solution doped with H_2O_2. The anodic branch of the PD curve represents the anodic dissolution of the alloy, while the cathodic branch represents the cathodic reaction of hydrogen evolution. It can be seen from Figure (6) that 2205 DSS exhibits a shift of both the anodic and cathodic branches towards lower corrosion current densities (i_{corr}) when normal saline solution was doped with (HP + albumin), indicating a decrease in anodic and cathodic kinetics [28, 29]. It should be noted here that (i_{corr}) values here are plotted in a logarithmic scale. In addition, the PD curves of the 2205 DSS in all three solutions show relatively large Tafel slopes, indicating high polarizability of the alloy in these environments.

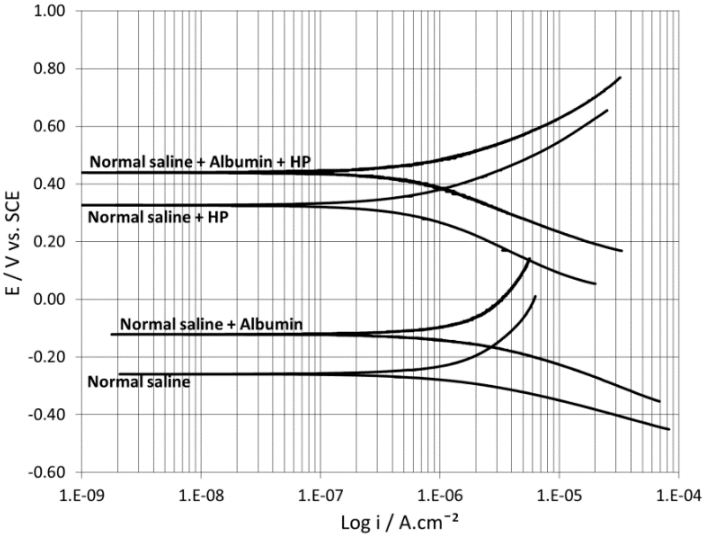

Figure 6: Typical potentiodynamic polarization curves of 2205 DSS after 1 hour immersion in the different electrolyte.

Figure (6) shows the increase in corrosion potential (Ecorr) of 2205 DSS when normal saline solution was doped with albumin, HP, and (HP + albumin). The values of Ecorr and Tafel slopes are listed in Table (1).

Table 1: Electrochemical parameters obtained from cyclic polarization tests after 1h immersion in saline solution and saline solution doped with HP, albumin, and (HP + albumin).

Electrolyte	E_{corr} (mV)	βa (mV/decade)	βc (mV/decade)
Normal saline	-260 ± 10	290 ± 16	95 ± 5.0
Normal saline + Albumin	-70 ± 15	260 ± 20	125 ± 13
Normal saline + HP	350 ± 10	112 ± 13	190 ± 13
Normal saline + Albumin + HP	420 ± 28	115 ± 7.0	170 ± 2.9

This shift in Ecorr as a result of the addition of HP to physiological environment under inflammatory conditions is similar to that reported for AISI 316 L stainless steel in 150 mM HP [30], CoCrMo-alloys in 0.5–30 mM HP solution and Ti-6Al-4V alloys in 8 mM HP solution [16], and nickel-free high-nitrogen steel FeCrMnMoN0.9 in 0.3-3 mM HP solution [17].

The corrosion rate in μm/year shown in Figure (7) was estimated by Faradic conversion of the i_{corr} (i.e. 1 μA/cm^2 corresponds to approximately 10 μm/year), supposing uniform corrosion of the metal (M) with the formation of M^{2+}. It was found that the corrosion rate of 2205 DSS (0.11 ± 0.007 μm/year) in normal saline solution was reduced to (0.04 ± 0.003 μm/year) due to the presence of HP in the electrolyte. The enhanced corrosion resistance could be related to the rapid formation of oxide film due to the presence of dissolved oxygen. These results are in good agreement with the results obtained from electrochemical impedance spectroscopy tests shown in Figure (5).

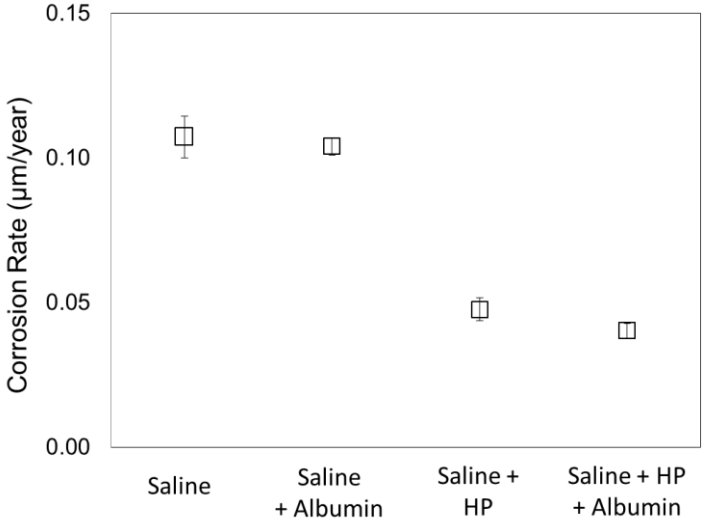

Figure 7: Corrosion rate of 2205 DSS in normal saline solution and normal saline solution doped with albumin and HP.

The shift of corrosion potential towards more positive values and the corresponding shift of corrosion current density towards lower values when normal saline solution was doped with HP, and to a lower extent upon the addition of human albumin, indicated that both solutions behaved like an anodic inhibitor. Anodic inhibitors act by reducing or blocking the anodic reaction and support the natural reaction of passivation of the metal surface as well as forming a film that is adsorbed on the metal. In general, the inhibitors react with the corrosion product resulting in a cohesive and insoluble film on the metal surface [31].

To the best of our knowledge, the corrosion resistance of 2205 DSS in physiological solutions containing HP has not been reported in the literature. The presence of HP has been previously reported for the AISI 316L stainless steel with a 150 mM solution and nickel-free, high-nitrogen austenitic steels (FeCrMnMoN0.9) in 3-30 mM HP solution [17]. The results of AISI 316L stainless steel indicated that HP caused a decrease in the corrosion resistance as a result of a decrease in the difference between open circuit potential and pitting potential. Radice et al. [17] found that the corrosion resistance of FeCrMnMoN0.9 was not affected upon addition of 3mM HP. Alternatively, the corrosion resistance was significantly decreased upon the addition of 3mM HP. They have related this behavior to the high content of nitrogen which enhances the pitting corrosion resistance of the steel. When dissolved in solid solution, nitrogen is found to consume H^+ ions therefore prevent the local pH drop, which allows for the protectiveness of the passive film. The higher amount of Cr, Mo and N in 2205 DSS may be responsible for the better corrosion resistance when compared to 316L austenitic stainless steel. This observation can be related to the Pitting Resistance Equivalent Number (PREN) which relates the resistance of stainless steels to localized corrosion to the concentration of alloying elements as follows [32].

$$PREN = \% Cr + 3.3\% Mo + 30\%N \quad (9)$$

PREN for 2205 DSS is 31, while that of 316L austenitic stainless steel is 25, indicating the former stainless steel performs better against localized corrosion than the latter one. Localized corrosion in stainless steels is the result of breaking of passivation film that can be accelerated by the presence of chloride ions. Improvement in resistance against localized corrosion, in Cl^- containing media, can be achieved if the corrosion product layer has chromium and molybdenum oxides and so acts as a passive layer. Cr helps in formation $Cr(OH)_3/Cr_2O_3$ while Mo forms MoO_2. Nitrogen in stainless steel is observed as a negatively charged ion. Presence of the negatively charged nitrogen ion on the metal surface under a passive film suppresses the adsorption of Cl^- ions on the passivating film or slowing down of their access to it. This process enhances stability of the passive film [32].

CONCLUSIONS

The aim of this work was to investigate the effect of human albumin and inflammatory conditions on the corrosion resistance of 2205 DSS. In order to simulate the inflammatory conditions in vitro, studies were conducted by addition of hydrogen peroxide (which is a reactive oxygen species found during inflammation) and albumin (which is the most typical protein in biological fluids). The experimental results reveal that the addition of 8 mL/L albumin or HP into normal saline solution significantly decreased the corrosion rate. It was found that HP enhanced the corrosion resistance of the stainless steel by increasing the thickness of the passive film. HP and to a lesser extent human albumin served as an anodic inhibitor as indicated by the potentiodynamic polarization results. These findings support the aim of this work by introducing duplex stainless steels as a promising alternative to austenitic stainless steel in biomedical applications.

REFERENCES

[1] G. Manivasagam, D. Dhinasekaran, and A. Rajamanickam, Biomedical Implants: Corrosion and its Prevention -A Review. Recent Patents on Corrosion Science, 2010. **2**: p. 40-54.

[2] J. Pan, C. Karlén, and C. Ulfvin, Electrochemical Study of Resistance to Localized Corrosion of Stainless Steels for Biomaterial Applications. Journal of The Electrochemical Society, 2000. **147**(3): p. 1021.
[3] R.W. Gregorutti, J.Enrique, F.Sives, and C.I. Elsnerc, Mechanical, electrochemical and magnetic behaviour of duplex stainless steel for biomedical applications. Materials Science and Technology, 2015. **31**(15): p. 1818-1824.
[4] C. XU, Y. ZHANG, G. CHENG, and W. ZHU, Corrosion and Electrochemical Behavior of 316L Stainless Steel in Sulfate-reducing and Iron-oxidizing Bacteria Solutions1 1 Supported by the National Natural Science Foundation of China (No.20576108). Chinese Journal of Chemical Engineering, 2006. **14**: p. 829-834.
[5] X. Lü, X. Bao, Y. Huang, Y. Qu, and H. Lu, Mechanisms of cytotoxicity of nickel ions based on gene expression profiles. Biomaterials, 2009. **30**(2): p. 141-8.
[6] F. Zhang, Y. Huang, Y. Zhang, and X. Lü, Screening and validation of nickel ion cytotoxicity biomarkers based on transcriptomic and proteomic technology. Regen Biomater, 2022. **9**: p. rbac073.
[7] G. Saulis, R. Rodaitė-Riševičienė, and R. Saulė, Cytotoxicity of a Cell Culture Medium Treated with a High-Voltage Pulse Using Stainless Steel Electrodes and the Role of Iron Ions. Membranes (Basel), 2022. **12**(2).
[8] H. Cheng, H. Luo, and X. Wang, Electrochemical corrosion and passive behavior of a new high-nitrogen austenitic stainless steel in chloride environment. Materials Chemistry and Physics, 2022. **292**: p. 126837.
[9] C. Yang, Q. Wang, Y. Ren, D. Jin, and D. Liu, Corrosion behavior of high nitrogen nickel-free austenitic stainless steel in the presence of artificial saliva and Streptococcus mutans. Bioelectrochemistry, 2021. **142**: p. 107940.
[10] Y. Qiao, X. Wang, L. Yang, X. Wang, J. Chen, Z. Wang, and H. Zhou, Effect of aging treatment on microstructure and corrosion behavior of a Fe-18Cr-15Mn-0.66N stainless steel. Journal of Materials Science & Technology, 2022. **107**: p. 197-206.
[11] K. Kumar, K. Anburaj, and J. Dhanasekar, Kinetics of Cr2N Precipitation and Its Effect on Pitting Corrosion of Nickel-Free High-Nitrogen Austenitic Stainless Steel. Journal of Materials Engineering and Performance, 2020. **29**: p. 1-9.
[12] I. Gurappa, Characterization of different materials for corrosion resistance under simulated body fluid conditions. Materials Characterization, 2002. **49**(1): p. 73-79.
[13] ASM Committee., Properties and Selection: Irons, Steels, and High-Performance Alloys. 1990: ASM International.
[14] M. Conradi, M. Schön, A. Kocijan, M. Jenko, and G. Julius Vancso, Surface analysis of localized corrosion of austenitic 316L and duplex 2205 stainless steels in simulated body solutions. Materials Chemistry and Physics, 2011. **130**(1): p. 708-713.
[15] Kocijan, A. and M. Conradi, The corrosion behaviour of austenitic and duplex stainless steels in artificial body fluids. Materiali in Tehnologije, 2010. **44**: p. 21-24.
[16] Dragus, L., et al., Effect of the inflammatory conditions and albumin presence on the corrosion behavior of grade 5 Titanium alloy in saliva biological solution. IOP Conference Series: Materials Science and Engineering, 2019. **572**(1): p. 012005.

[17] L. Dragus, L. Benea, N. Simeonescu, and A. Ravoi, Corrosion resistance of the nickel-free high-nitrogen steel FeCrMnMoN0.9 under simulated inflammatory conditions. J Biomed Mater Res B Appl Biomater, 2021. **109**(6): p. 902-910.
[18] C. Alexander, B. Tribollet, and M. Orazem, Contribution of Surface Distributions to Constant-Phase-Element (CPE) Behavior: 1. Influence of Roughness. Electrochimica Acta, 2015. **173**.
[19] H. Luo, C. Dong, X. Cheng, K. Xiao, and X. Li, Electrochemical Behavior of 2205 Duplex Stainless Steel in NaCl Solution with Different Chromate Contents. Journal of Materials Engineering and Performance, 2012. **21**(7): p. 1283-1291.
[20] M. Fathy, M. Bayoumi, A. W. Ghanem, Effect of Nitrogen on the Corrosion Behavior of Austenitic Stainless Steel in Chloride Solutions. Modern Applied Science, 2015. **9**: p. 119.
[21] H. Mraied, W. Cai, and A.A. Sagüés, Corrosion resistance of Al and Al–Mn thin films. Thin Solid Films, 2016. **615**: p. 391-401.
[22] S. Gudić, A. Nagode, K. Šimić, L. Vrsalović, and S. Jozić, Corrosion Behavior of Different Types of Stainless Steel in PBS Solution. Sustainability, 2022. **14**: p. 8935.
[23] King, A.D., N. Birbilis, and J.R. Scully, Accurate Electrochemical Measurement of Magnesium Corrosion Rates; a Combined Impedance, Mass-Loss and Hydrogen Collection Study. Electrochimica Acta, 2014. **121**: p. 394-406.
[24] G. Bland, A.D. King, N. Birbilis, and J.R. Scully, Assessing the Corrosion of Commercially Pure Magnesium and Commercial AZ31B by Electrochemical Impedance, Mass-Loss, Hydrogen Collection, and Inductively Coupled Plasma Optical Emission Spectrometry Solution Analysis. Corrosion, 2015. **71**(2): p. 128-145.
[25] A. Pardo, S. Feliu, M. C. Merino, R. Arrabal, and E. Matykina, Electrochemical Estimation of the Corrosion Rate of Magnesium/Aluminium Alloys. International Journal of Corrosion, 2010. **2010**.
[26] Petty, R.L., A.W. Davidson, and J. Kleinberg, The Anodic Oxidation of Magnesium Metal: Evidence for the Existence of Unipositive Magnesium1,2. Journal of the American Chemical Society, 1954. **76**(2): p. 363-366.
[27] D. Liu, X. Xie, J. Roscher, and R. Holze, comparative study of the corrosion stability of dental amalgams with electrochemical impedance measurements. Materials and Corrosion, 2020. **71**(6): p. 949-955.
[28] A.D. Sudholz, K. Gusieva, X.B. Chen, B.C. Muddle, M.A. Gibson, and N. Birbilis,Electrochemical behaviour and corrosion of Mg–Y alloys. Corrosion Science, 2011. **53**(6): p. 2277-2282.
[29] C. Gusieva, C. Davies, J. R. Scully, and N. Birbilis, Corrosion of magnesium alloys: the role of alloying. International Materials Reviews, 2015. **60**(3): p. 169-194.
[30] I. Milošev, J. Hmeljak, and A. Cör, Hyaluronic acid stimulates the formation of calcium phosphate on CoCrMo alloy in simulated physiological solution. J Mater Sci Mater Med, 2013. **24**(3): p. 555-71.
[31] A. Galio, and C. Dariva, Corrosion Inhibitors – Principles, Mechanisms and Applications. 2014. p. 365-380.
[32] A.Singh, V. Chaudhary, and A. Sharma, Electrochemical Studies of Stainless Steel Corrosion in Peroxide Solutions. Portugaliae Electrochimica Acta, 2012. **30**: p. 99-109.